

# 基于相关与时耗复合维归约的弧焊电源动特性自适应在线监测

高理文<sup>1,2</sup>, 薛家祥<sup>1</sup>, 陈辉<sup>1</sup>, 王瑞超<sup>1</sup>, 林放<sup>1</sup>

(1. 华南理工大学机械与汽车工程学院, 广州 510640; 2. 广州中医药大学信息技术学院, 广州 510006)

摘要: 提出了相关与时耗复合维归约方法, 可实现多种弧焊电源动特性自适应在线监测。其核心思想是从一个大的特征库中选出最贴近监测对象的若干特征。该方法充分考虑特征间的相关性, 以及在线监测的时效性。搭建了较为完善的焊接试验数据采集平台, 共采集 189 次焊接过程的电压电流数据作为样本, 并以人工评定结果作为文中维归约方法教师信号, 即类的标签。随机选择 150 个样本组成训练集, 剩余 39 个组成测试集。运用文中维归约方法的寻找最优的特征子集。结果表明, 找到的最优特征子集的自动化评定准确率达 97.435 9%, 接近应用要求。

关键词: 弧焊电源; 在线监测; 维归约

中图分类号: TG409 文献标识码: A 文章编号: 0253-360X(2012)04-0017-04



高理文

## 0 序 言

在实际生产应用中, 对弧焊电源动特性好坏的评定, 长期以来, 由有经验的焊工经试焊后做出评价。所谓动特性好, 一般指焊接过程稳定、飞溅小、焊缝成形好。由于这种方法具有很大的个人主观成分, 并未获得推广。国内外相关学者已开始针对特定的某种弧焊电源开展自动化测评的研究。1999年, 张晓因<sup>[1]</sup>研究探索了 CO<sub>2</sub> 弧焊电源动特性的评定方法。以统计分析和小波分析从弧焊电信号中提取特征, 并通过模糊逻辑推理进行自动化评定。2000年, Zhu 等人<sup>[2]</sup>提出了一个非线性模型, 用以分析弧焊电源的动态行为, 并通过试验对照, 证明了该方法的正确性。2003年, 杨立军等人<sup>[3]</sup>对 CO<sub>2</sub> 焊短路过程动特性与外特性的关系进行研究。2009年, Wang 等人<sup>[4]</sup>建立了仿真模型, 分析逆变式弧焊电源的动特性, 并经过试验验证。然而能投入应用的弧焊电源动特性在线监测技术未见报道。一方面, 弧焊过程复杂, 难以实现实用的自动化在线监测技术。更重要的是弧焊电源的基本原理、主电路结构、材料等各方面均已得到长足发展, 并且保持良好的

势头。面对型号规格日新月异的弧焊电源, 传统的研究思路陷入了困境。

文中引入维归约的理论, 破解该难题。其基本思路是收集足够多与弧焊电源动特性有关的特征, 构造一个足够大并且支持扩充的特征库。当面对特定某类或者某型号弧焊电源时, 以试验为判断依据, 从特征库中自动化地寻找出既能有效预测评定该电源动特性优劣, 又能满足在线应用时耗要求的若干特征。

维归约概念源于数据挖掘的范畴<sup>[5]</sup>, 就是从一组给定的特征集合中构造出一个具有代表性的特征子集, 使其保留原特征集的大部分有用的数据信息, 从而达到降低特征空间维数的目的。West<sup>[6]</sup>在基因工程研究的例子表明, 有时特征维度甚至多于数据样本数目, 必须降维。现有的维归约方法主要是解决特征冗余和相关的问题, 没有时耗的概念。而在多样化弧焊电源在线监测的应用中, 相关与时耗耦合的问题不可回避。首先, 特征之间具有相关性。其次, 提取每个特征都需要消耗时间。而采用训练好的分类器分类所消耗的时间往往非常小, 并且较为固定, 文中拟采用的支持向量机在预测时就非常快; 所以, 被选出的若干特征的时耗的总和就决定了延时的长短。因此该问题就转化为在满足时耗总和小于某个设定值的条件下, 从相互相关的大量特征中, 寻找出分类评定效果最佳的若干特征。文中研究团队深入钻研, 成功探索出支持自适应在线监测

收稿日期: 2011-08-26

基金项目: 国家自然科学基金资助项目(50875088); 广东省科技计划资助项目(2010B010700001); 番禺区科技计划资助项目(2010-Z-22-4); 黄埔区科技计划资助项目(1021)

的相关与时耗复合维归约方法.

## 1 相关与时耗复合维归约方法

该方法的详细过程如下.

步骤 1: 包含. 它包括两个子步骤.

步骤 1.1: 先判断当前的特征子集( currentsubset, CS) 和上一次循环执行步骤 1 时的特征子集是否相同, 若是, 则结束.

步骤 1.2: 加 1 个特征. 先按下式, 找出最优新特征  $j$ . 然后再把它加入到当前特征中来, 并记下这个新特征.

$$\arg \text{Max}_j \sum_{i \in \text{CS}} T(i) + \sum_{i \in \text{CS}} T(i) < t_{\text{AMTC}} (\text{Value}(\text{CS} \cup \{j\})) \quad (1)$$

式中:  $\arg \text{Max}_A(B)$  是指求出在满足约束条件  $A$  的情况下, 使得  $B$  取得最大值的参数  $j$ ; CS 指当前特征子集;  $t_{\text{AMTC}}$  是指允许消耗的最大时间.  $T(k)$  函数为返回特征  $k$  的时耗, 也就是从原始物理信号序列中提取特征  $k$  所要消耗的时间值.  $\text{Value}(x)$  函数为返回特征集  $x$  的自动评定准确率, 其过程是先查询缓冲区( cache) 是否有记录了特征集  $x$  及  $\text{Value}(x)$ , 若有, 直接读出. 否则, 把特征集  $x$  输入到支持向量机, 基于训练集, 采用交叉检验的方法, 修正支持向量机的内部参数, 然后, 对于测试集, 计算其自动评定的准确率. 最后把  $x$  及  $\text{Value}(x)$  存入缓冲区, 并返回  $\text{Value}(x)$ .

步骤 2: 检验. 它包括如下子步骤.

步骤 2.1: 在当前特征子集 CS 中找 1 个最不重要的特征  $u$ , 方法为

$$\arg \text{Max}_{u \in \text{CS}} (\text{Value}(\text{CS} \cup \{u\})) \quad (2)$$

即找到一个特征  $u$ , 与其它任一特征相比, 删除  $u$  后所得特征子集的 Value 的减少量最小.

步骤 2.2: 计算 CS 删除  $u$  所得特征子集的 Future<sub>1</sub>, 即  $\text{Future}(\text{CS} - \{u\})$ ; 在集合 CS 中删掉除  $u$  以外的任意一个特征  $v$ , 计算 Future<sub>2</sub>, 即  $\text{Future}(\text{CS} - \{v\})$ ; 比较 Future<sub>1</sub> 与 Future<sub>2</sub> 的大小, 若  $\text{Future}_2 > \text{Future}_1$ , 则将集合(  $\text{CS} - \{v\}$ ) 存入候选队列; 按上述规则逐个找出特征  $v$ , 把所有的集合(  $\text{CS} - \{v\}$ ) 都存入候选队列;

Future(  $x$ ) 的计算方法主要是把库中所有特征, 按时耗  $T(k)$  从小到大排列, 形成一个时耗队列; 从队首选取不属于特征集  $x$  的特征填充至特征集  $x$  中, 当特征集  $x$  的总时耗大于总时耗限制值  $t_{\text{AMTC}}$  则停止; 所述 Future 即为所增加的特征的个数.

步骤 2.3: 判断  $u$  是不是刚才加入的  $j$ , 若是, 不

删除  $u$ , 转向步骤 1, 否则, 从 CS 真正删除  $u$ , 更新 CS, 然后转向步骤 3.

步骤 3: 排除. 它包括如下子步骤.

步骤 3.1: 在当前特征子集 CS 中找 1 个最不重要的特征  $y$ . 与步骤 2.1 寻找  $u$  的方法相同.

步骤 3.2: 把所有(  $\text{CS} - \{y\}$ ) 都存入候选队列; 同步步骤 2.2.

步骤 3.3: 如果能在缓存区中找到一个特征子集( othersubset, OS) 满足

$$\left. \begin{aligned} \text{Value}(\text{OS}) &\geq \text{Value}(\text{CS} - \{y\}) \\ \text{Future}(\text{OS}) &\geq \text{Future}(\text{CS} - \{y\}) \end{aligned} \right\} \quad (3)$$

则不删除  $y$ , 直接转向步骤 1.

步骤 3.4: 从 CS 中真正删除  $y$ , 更新 CS.

步骤 3.5: 如果 CS 中只剩下一个特征, 转向步骤 1, 否则, 转向步骤 3.

上述步骤 1 至步骤 3 组成了第一轮复合维归约. 第二及以后轮次, 从候选队列中取 1 个特征集作为初始集合, 按上述步骤 1 至步骤 3 删除步骤 2.2 和步骤 3.2 后得到的流程, 进行复合维归约. 当候选队列中的集合全部计算完毕, 也就是所有轮次计算完毕之后, 在缓冲区 cache 中找到 Value 最大的特征子集, 该集合就是复合维归约的最终结果.

## 2 试验验证与分析

### 2.1 原始数据采集

文中团队长期从事熔极气体保护焊的自动化检测研究, 搭建了如图 1 所示的试验平台. 采用该平台, 对 3 台焊机( NBC250, NBC350, 自行研制的多功能数字化焊机) 进行了实测评定. 气体流量为 16 L/min, 随机选用直径为 1.0, 1.2 和 1.6 mm 的焊丝. 其焊丝伸出长度为 12 mm, 试件为 Q235 钢板. 试验平台中的小波分析仪配置了电压传感器和电流

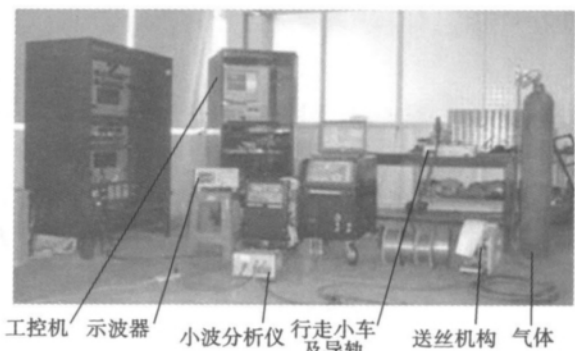


图 1 焊接试验平台

Fig. 1 Picture of testing platform

霍尔传感器,用以采集电压电流信号。共进行了189次焊接试验。对于每个焊接过程,采集其电压电流信号并存储为1个数据样本,并由专业焊工根据焊接现场的弧光闪烁变化程度、电弧声柔和程度、飞溅大小、焊缝光洁程度等因素,人工进行综合评测,把弧焊电源的动特性优劣分别归入1(合格)、0(不合格)两个等级之一,以此作为文中维归约方法的教师信号,即类的标签。随机选择150个样本组成训练集,剩余39个组成测试集。

2.2 特征库构建

文中方法的核心思想是从特征库中选择出最佳的若干特征。因此必须构建具有一定规模,覆盖全面的特征库。当前,文中研究团队已探索出54个特征:(1)燃弧时间平均值;(2)燃弧时间变异系数;(3)短路时间平均值;(4)短路时间变异系数;(5)短路时刻电流平均值;(6)短路时刻电流变异系数;(7)峰值电流平均值;(8)峰值电流变异系数;(9)燃弧能量平均值;(10)燃弧能量变异系数;(11)燃弧功率平均值;(12)燃弧功率变异系数;(13)短路能量平均值;(14)短路能量变异系数;(15)短路功率平均值;(16)短路功率变异系数;(17)燃弧电阻平均值;(18)燃弧电阻变异系数;(19)短路电阻平均值;(20)短路电阻变异系数;(21)周期功率平均值;(22)周期功率变异系数;(23)周期电阻平均值;(24)周期电阻变异系数;(25)断弧率;(26)正态周期重复率;(27)正态周期重复率-系数×断弧率;(28)瞬时短路频率;(29)短路频率(包括正常和瞬时);(30)平均电流;(31)平均电压;(32)短路中期电流上升率平均值;(33)短路中期电流上升率变异系数;(34)电压自相关函数峰值间距变异系数;(35)电流自相关函数峰值间距变异系数;(36)功率自相关函数峰值间距变异系数;(37)电阻自相关函数峰值间距变异系数;(38)正常短路频率;(39)周期平均值;(40)周期变异系数;(41)各周期燃弧时间与短路时间之比的平均值;(42)各周期燃弧时间与短路时间之比的变异系数;(43)燃弧时间平均值与短路时间平均值之比;(44)燃弧功率平均值与短路功率平均值之比;(45)燃弧能量平均值与短路能量平均值之比;(46)平均燃弧电压;(47)平均燃弧电流;(48)平均短路电压;(49)平均短路电流;(50)最大电压;(51)短路末期功率平均值;(52)短路末期功率变异系数;(53)起弧平均功率;(54)起弧功率变异系数。这些特征通过统计和信号处理的方法从焊接过程的电压电流数据中提取。一些特征比如涉及到“燃弧”或“短路”就需要通过阈值方法检测电压值,以判断任一信号点是处于“燃弧”还是

“短路”状态。由于篇幅的关系,文中只列出所采集的两个焊接过程电信号数据样本的特征值情况,见表1。两个样本的电压电流波形图如图2,图3所示。其中样本1的电压电流波形一致性很好,无瞬时短路,无断弧。而与之对应的弧焊电源的动特性被综合评定为合格。样本2的电压电流波形一致性比较差,有瞬时短路,动特性被综合评定为不合格。

表1 样本特征值数据  
Table 1 Eigen values of samples

特征 编号	特征值 $n$		特征 编号	特征值 $n$	
	样本1	样本2		样本1	样本2
1	20.754 46	19.801 43	28	0	10
2	0.118 888	0.678 375	29	27.5	35
3	14.959 82	8.646 479	30	128.317 8	271.362 6
4	0.092 951	0.797 049	31	16.965 52	23.015 12
5	59.351 22	207.083 2	32	13 985.09	-11 150.8
6	0.144 745	0.269 126	33	0.033 86	7.701 026
7	287.187 2	371.102 9	34	0.650 142	1.487 042
8	0.017 188	0.322 496	35	0.072 25	0.607 684
9	35 853.91	142 900	36	0.678 887	1.367 779
10	0.111 604	0.723 292	37	0.638 731	1.479 592
11	1 755.594	6 761.443	38	27.5	24.5
12	0.158 175	0.299 42	39	723.127 3	564.956 5
13	16 355.97	26 088.74	40	0.034 528	0.513 551
14	0.119 789	1.144 024	41	1.399 012	14.311 41
15	1 094.95	2 536.931	42	0.086 986	1.820 265
16	0.083 684	0.416 367	43	1.387 347	2.290 115
17	0.487 061	0.135 331	44	1.603 355	2.665 205
18	0.122 794	0.189 584	45	2.192 098	5.477 461
19	0.023 884	0.027 455	46	25.714 79	29.645 36
20	0.031 986	0.274 948	47	66.057 18	235.512 2
21	1 457.174	5 812.143	48	4.827 257	8.044 946
22	0.074 801	0.358 731	49	214.694 8	352.307 6
23	0.296 799	0.098 206	50	31.317 37	40.696 66
24	0.111 842	0.365 621	51	3 121.134	4 931.051
25	0	0	52	0.098 264	0.427 431
26	0.699 449	0.173 331	53	4 397.222	6 336.575
27	0.699 449	0.173 331	54	0.088 034	0.342 114

2.3 复合维归约结果

按复合维归约的方法,基于训练集,不断地探寻能以最大正确率自动评定测试集各样本等级的特征子集。经过23轮的计算,程序结束。其中,符合时耗要求的最佳的特征子集在第18轮中计算出来,共9个特征,该子集对39个测试样本的等级进行自动评定,38个的结果均和人工评价一致,其自动评定准确率为97.435 9%,已接近应用要求。这9个特征

编号为 6 10 14 19 30 34 42 48 50.

### 3 结 论

(1) 面对电焊机制造技术的飞速发展,弧焊电源新型号的不断涌现,传统逐个研究建立监测系统的思路已难以实行.文中提出了基于相关与时耗复合维归约方法,有效破解该困局,可实现多种弧焊电源动特性自适应在线监测.

(2) 对 CO<sub>2</sub> 弧焊电源应用文中方法进行试验.共进行了 189 次焊接试验.经过训练学习后进行测试,统计得到自动判定准确率为 97.435 9%.该值已接近实际应用的要求,充分说明文中所提出的复合维归约方法切实可行.

#### 参考文献:

- [1] 张晓园. CO<sub>2</sub> 弧焊电源动特性评定新方法的研究[D]. 广州: 华南理工大学, 1999.
- [2] Zhu Jinhong, Liang Wenlin, Shi Yaowu. Study on the dynamic process of arc welding inverter[C]// Proceedings of the Third International Power Electronics and Motion Control Conference, Beijing, 2000: 308 - 311.
- [3] 杨立军, 李俊岳, 李 桓, 等. CO<sub>2</sub> 焊短路过程动特性与外特性的关系[J]. 焊接学报, 2003, 24(2): 31 - 34.  
Yang Lijun, Li Junyue, Li Huan, et al. Relation of dynamic and output characteristic in CO<sub>2</sub> short circuit arc welding[J]. Transactions of the China Welding Institution, 2003, 24(2): 31 - 34.
- [4] Wang Chunfang, Wang Zhaoan, Xu Qinshao. Study on dynamic characteristics of inverter arc welding power supply based on double-loop control[C]// Proceedings of 6th International Power Electronics and Motion Control Conference, Wuhan, 2009: 1609 - 1612.
- [5] Thangavel K, Pethalakshmi A. Dimensionality reduction based on rough set theory: A review[J]. Applied Soft Computing Journal, 2009, 9(1): 1 - 12.
- [6] West M. Bayesian factor regression models in the "large p, small n" paradigm[J]. Bayesian Statistics, 2003, 7: 723 - 732.

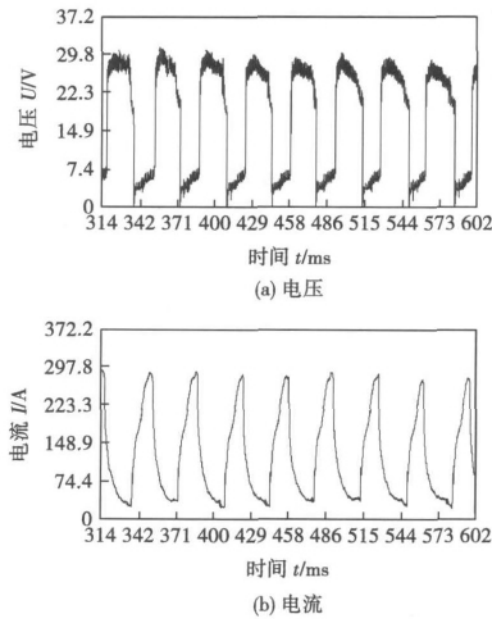


图 2 样本 1 电压电流波形  
Fig. 2 Voltage and current waveform of sample 1

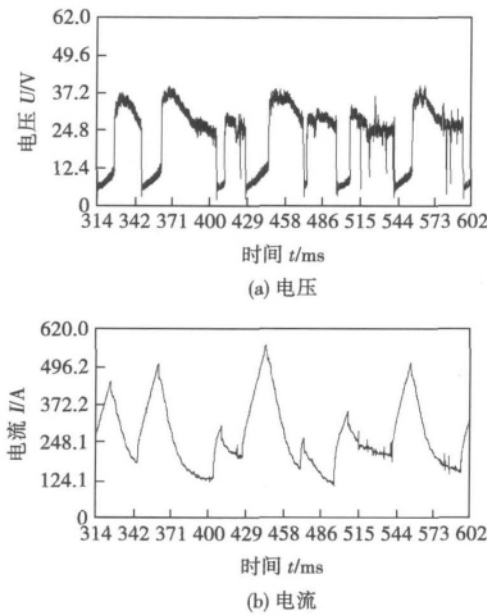


图 3 样本 2 电压电流波形  
Fig. 3 Voltage and current waveform of sample 2

作者简介: 高理文,男,1981 年出生,博士研究生,讲师.主要从事智能化检测研究.发表论文 17 篇. Email: glwemail@163.com

通讯作者: 薛家祥,男,教授. Email: mejiaxue@scut.edu.cn

## MAIN TOPICS ,ABSTRACTS & KEY WORDS

**Prediction algorithm of weld seam deviation based on RBF neural network** GAO Xiangdong<sup>1</sup> , MO Ling<sup>1</sup> , YOU Deyong<sup>1</sup> , KATAYAMA Seiji<sup>2</sup> ( 1. Faculty of Electromechanical Engineering , Guangdong University of Technology , Guangzhou 510006 , China; 2. Joining and Welding Research Institute , Osaka University , Osaka 567-0047 , Japan) . pp 1 - 4

**Abstract:** An algorithm was proposed to predict the weld seam deviation in high-power fiber laser ( maximal laser power 10kW) welding of type 304 austenitic stainless steel. A high-speed camera was employed to capture the infrared-images of the molten pool in welding process. The eigenvectors such as keyhole centroid , keyhole configuration parameter , heat accumulation effect parameter and so on reflected the deviations between the laser beam and the weld seam position , which were applied as the inputs of a RBF( radial basis function) neural network , and a RBF neural network model was established to predict the weld deviations. The eigenvectors of weld deviations were sampled to train the prediction model , and the established prediction model was tested by the fiber laser welding data. Experimental results showed that the founded model could predict the deviations between the laser beam and the weld seam position during the high-power fiber laser welding.

**Key words:** high-power fiber laser welding; RBF neural network; weld seam deviations; prediction

**Effect of magnetic-control arc sensor on weld width of submerged arc welding** HONG Bo , LI Lin , LI Xiangwen , MA Jinhai ( Mechanical Engineering College , Xiangtan University , Xiangtan 411105 , China) . pp 5 - 8

**Abstract:** Based on the magnetic-control arc sensor model , the mathematical model of weld for thin wire submerged arc welding was established to track seam. By using the mathematical model , the variation of weld width at the transverse alternating magnetic field was studied. The influencing curve of excitation frequency and current on weld width was obtained by experiments , and the simulation results and that of experiments were compared. The results showed that the weld width increased with increase of excitation current and decrease of the excitation frequency. The simulation results are basically consistent with the experimental results , which verifies the correctness of the model. The studies will provide the necessary theoretical guidance for the designment and development of the magnetic-control sensor and seam tracking system for thin wire submerged arc welding.

**Key words:** submerged arc welding; mathematical model; seam tracking; weld width

**Application of control parameter in sinusoid modulation pulsed MIG welding of aluminum alloy** WEI Zhonghua , LONG Peng , CHEN Xiaofeng , XUE Jiayang ( School of Mechanical & Automotive Engineering , South China University of Technology , Guangzhou 510640 , China) . pp 9 - 12

**Abstract:** Based on the difficulties in welding of light material like aluminum alloy , which required low energy input and other requirements , the control parameter relationship formula was established for sinusoid modulation pulsed MIG welding of aluminum , and experiments were used to validate its correctness and practicability. Due to the characteristics of sinusoidal waveform such as infinite derivative continuity , eternal periodicity and less controlled variable , the modulation pulse waveform can realize to effectively and precisely regulate welding energy , and the stable and high quality fish scale weld seam can be obtained. While experiments indicated that the change range of  $m$  value in the relationship formula is from 2 to 3. There are advantages in sinusoid modulation pulse MIG welding such as wider parameters matching range , less interference from external working environmental factors , which lays the theoretical foundation for the parameter unification exploitation in the sinusoid modulation pulsed MIG welding process.

**Key words:** pulsed welding; sinusoid modulation; periodicity; stability

**Influence of powder-feeding mode on microstructure of WC reinforced composite coating** SONG Zili<sup>1</sup> , DU Xiaodong<sup>1</sup> , LI Lianying<sup>1</sup> , WANG Jiaqing<sup>2</sup> ( 1. School of Materials Science and Engineering , Hefei University of Technology , Hefei 230009 , China; 2. Institute of Materials , Anhui Electric Power Research Institute , Hefei 230009 , China) . pp 13 - 16

**Abstract:** WC reinforced Ni-based composite coating was prepared by using plasma surfacing process with two different power-feeding modes of synchronous feeding and back feeding. The microstructure , phase structure and chemical compositions were analyzed by scanning electron microscopy ( SEM) , X-ray diffractometer ( XRD) and energy dispersive spectrometer ( EDS) . Results showed that the microstructure consists of WC particles embedded in hypoeutectic matrix. Compared with synchronous feeding , less dissolution of WC , less primary phases WC ,  $W_2C$  with finer microstructure and greater concentration gradient of elements were observed in the composite coating with back-feeding process.

**Key words:** WC composite coating; power-feeding mode; dissolution; microstructure

**Adaptive online detection on dynamic characteristics of arc welding power supply based on complicated dimensionality reduction of correlation and time consumption** GAO Liwen<sup>1,2</sup> , XUE Jiayang<sup>1</sup> , CHEN Hui<sup>1</sup> , WANG Ruichao<sup>1</sup> , LIN Fang<sup>1</sup> ( 1. School of Mechanical and Automotive Engineering , South China University of Technology , Guangzhou 510640 , China; 2. College of Information Technology , Guangzhou University of Chinese Medicine , Guangzhou 510006 , China) . pp 17 - 20

**Abstract:** A complicated dimensionality reduction of correlation and the time consumption was put forward , which real-

ized the adaptive online detection on different dynamic characteristics of arc welding power supply. The main idea of this method was to select some certain features from the complete feature set which were the closest to the detection targets. The correlation among features and the efficiency of the online detection were fully taken into account in the use of this method. A perfect welding data collection platform was set up , the samples of the voltage and current data were collected in the 189 welding processes , and the artificial evaluation results were taken as the teacher's signals , namely the cluster labels , in the dimension reduction. 150 samples were randomly selected as training set , while the remaining 39 samples were used as the test suite. The results of the experiments showed that the automatic evaluation accuracy of the chosen one reached 97.435 9% and satisfied the application requirements when the optimal feature subset was chosen based on the dimension reduction method.

**Key words:** arc welding power supply; online detection; Dimensionality reduction

**Application of image morphology in detection of initial welding position** WANG Jian , WEI Shanchun , LIN Tao , CHEN Shanben ( Intelligentized Robotic Welding Technology Laboratory , Shanghai Jiao Tong University , Shanghai 200240 , China) . pp 21 – 24

**Abstract:** The image morphology was introduced to detect the initial welding position of straight welding seam. The straight seam image was acquired by using a small CCD camera. The erosion edge detection algorithm was used to process the image , which could maintain the key information and eliminate other interference. Finally the initial welding position was obtained by filter with directional liner structure elements and Hough transformation. The whole processing is very intuitionistic , simple and fast. In addition , it's higher self-adaptability , higher process accuracy and stronger robustness. This research can meet the need of practical work , and lay a good foundation for the guidance of initial welding position.

**Key words:** image morphology; structure elements; initial welding position

**FEM of welding stress in AH36 steel plate with different welding parameters** WU Mingfang<sup>1</sup> , LU Xuedong<sup>1</sup> , CEN Yue<sup>2</sup> , WANG Huan<sup>2</sup> ( 1. Department of Material Science and Engineering , Jiangsu University of Science and Technology , Zhenjiang 212003 , China; 2. HuDong ZhongHua Ship Building Company Limited , Shanghai 200129 , China) . pp 25 – 28

**Abstract:** With the three-dimensional finite element and experimental method , the residual stress in the AH36 steel plate of 6 mm in thickness under different welding conditions was studied in this paper. The results showed that the peak stress , which was the largest with the combined welding method , was related with the welding heat input under the same cooling condition. The longitudinal stress distribution varies with cooling conditions for the same welding process. Compared with the conventional welding , the welding residual stress distribution , especially in the peak residual tensile stress , was improved by water cooling. An experiment with the same parameters was carried out to verify the finite element simulation results. The experimental results

are consistent with the numerical results , which indicates that the welding stress evolution under different welding conditions can be simulated with the three-dimensional finite element simulation technology , and provide the basis of the control of welding residual stress.

**Key words:** AH36 steel; residual stress; water cooling; finite element method

**Theoretical analysis for output characteristics of soft-switching arc welding inverter** WANG Ruichao , XUE Jiaxiang ( School of Mechanical and Automotive Engineering , South China University of Technology , Guangzhou 510641 , China) . pp 29 – 32

**Abstract:** Through the analysis of phase-shifted soft-switching full-bridge power converter characteristics , a soft-switching arc welding power system topology of peak-current mode control is proposed. The full-bridge model of arc welding power is equated to Buck model using small-signal analysis method. Buck model works in continuous conduction mode or discontinuous conduction mode under different load conditions. Based on circuit theory , the boundary points of static characteristics in one PWM working process cycle of phase-shifted full-bridge zero-voltage-switch are analyzed with theoretical derivation. The adjustment range of welding parameters is directly determined by the boundary curves of arc welding power output characteristics. Thus , it can achieve the required output characteristics of arc welding power source by using different control strategies.

**Key words:** soft-switching arc welding power; equivalent model; boundary of output characteristics; peak-current mode control

**Comparison of microstructure and properties of deposited metal under DC longitudinal/transverse magnetic field**

SU Yunhai , LI Lecheng , LIU Zhengjun ( School of Materials Science and Engineering , Shenyang University of Technology , Shenyang 110780 , China) . pp 33 – 36

**Abstract:** The Fe5 alloy was overlaid on low carbon steel by plasma arc surfacing with DC longitudinal magnetic field and DC transverse magnetic field , respectively. The magnetic field current and surfacing current were changed during surfacing. After PLA with magnetic field , the OM , wear loss test , micro-hardness test were used to analyze the effect of magnetic field style on microstructure and properties of deposited metal. The difference and mechanisms of magnetic field style and parameters on properties and microstructure of deposited metal were researched. The results indicate that the introduced longitudinal and transverse magnetic field can increase the nucleation ratio of hard phase and improve the properties of deposited metal. The distribution of hard phase is random under the transverse magnetic field , but it is hexagonal under longitudinal magnetic field. So the effect of DC longitudinal magnetic field is better than that of DC transverse magnetic field on wear resistance of surfacing layer , the effect of DC longitudinal magnetic field is worse than that of DC transverse magnetic field on hardness of surfacing layer.

**Key words:** plasma arc surfacing; DC transverse magnetic field; DC longitudinal magnetic field; Fe-based alloy; microstructure and properties